

Vision Language Modeling of Content, Distortion and Appearance for Image Quality Assessment

Fei Zhou, Zhicong Huang, Tianhao Gu, and Guoping Qiu

Abstract—The visual quality of an image is confounded by a number of intertwined factors including its semantic content, distortion characteristics and appearance properties such as brightness, contrast, sharpness, and colourfulness. Distilling high level knowledge about all these quality bearing attributes is crucial for developing objective Image Quality Assessment (IQA). While existing solutions have modeled some of these aspects, a comprehensive solution that involves all these important quality related attributes has not yet been developed. In this paper, we present a new blind IQA (BIQA) model termed Self-supervision and Vision-Language supervision Image Quality Evaluator (SLIQUE) that features a joint vision-language and visual contrastive representation learning framework for acquiring high level knowledge about the images semantic contents, distortion characteristics and appearance properties for IQA. For training SLIQUE, we have developed a systematic approach to constructing a first of its kind large image database annotated with all three categories of quality relevant texts. The Text Annotated Distortion, Appearance and Content (TADAC¹) database has over 1.6 million images annotated with textual descriptions of their semantic contents, distortion characteristics and appearance properties. The method for constructing TADAC and the database itself will be particularly useful for exploiting vision-language modeling for advanced IQA applications. Extensive experimental results show that SLIQUE has superior performances over state of the art, demonstrating the soundness of its design principle and the effectiveness of its implementation.

I. INTRODUCTION

Developing Image Quality Assessment (IQA) models that correlate well with human perceptual judgments is difficult. No-Reference Image Quality Assessment (NR-IQA), also known as blind IQA (BIQA), is more useful in real-world scenarios since it does not require any reference to quantify

This work was supported in part by the National Natural Science Foundation of China under Grant 62271323 and U22B2035, in part by Guangdong Basic and Applied Basic Research Foundation under Grant 2023A1515012956 and 2023B1212060076, and in part by the Shenzhen Research and Development Program under Grant JCYJ20220531102408020 and KJZD20230923114209019. (*Corresponding author: Guoping Qiu.*)

Fei Zhou is with College of Electronic and Information Engineering, Shenzhen University, Shenzhen 518060, China and also with Guangdong Provincial Key Laboratory of Intelligent Information Processing, Shenzhen 518060, China. (e-mail: flying.zhou@163.com).

Zhicong Huang and Tianhao Gu are with College of Electronic and Information Engineering, Shenzhen University, Shenzhen 518060, China, also with Peng Cheng Laboratory, Shenzhen 518000, China. (e-mail: 2110436021@email.szu.edu.cn; 2300432037@email.szu.edu.cn).

Guoping Qiu is with the College of Electronic and Information Engineering, Shenzhen University, Shenzhen 518060, China and also with the School of Computer Science, University of Nottingham, Nottingham NG8 1BB, UK. (e-mail: guoping.qiu@nottingham.ac.uk).

¹TADAC database will be made publicly available.

the human-perceivable image quality. However, lacking reference information also makes developing BIQA models more challenging.

Although deep learning-based BIQA methods have significantly advanced state of the art, the key challenge of lacking large labeled training dataset still remains. Existing IQA databases are generally inadequate in size. A common strategy to overcoming this difficulty is to train a model using synthetic images with artificial distortion and then regress the model to a small-scale target BIQA database. However, image distortions in the real world are complex and it is very difficult to simulate all possible real world scenarios. Another approach is to use self-supervised learning (SSL) [4], [13], [50] to overcome the lack of sufficient training data, as SSL is able to leverage large amount of unlabeled data. A much more fundamental challenge in BIQA is that human perception of quality can vary with the content of the image [39], thus image quality is not only affected by distortion but is also closely tied to image content. Therefore content and distortion **confound** the image quality assessment problem. The fact that it is very difficult to distinguish genuine image features such as high frequency signals from distortion such as compression artifacts makes developing BIQA models even harder.

Human have the ability to effortlessly recognize the scene and objects depicted in an image, almost unaffected by distortions. Although it is still unknown how the brain processes content and distortion, it is reasonable and useful to assume, conceptually at least, that it processes the content and the distortion with separately mechanisms. Fig. 1 shows some example images of different contents and distortions. Taking Fig. 1(b) for example, we first notice the scene (city) and then on close inspection we see the image is noisy. Other images can also be separated into content and distortion. Based on these examples, it seems to make reasonable sense to regard visual quality assessment as consisting of recognising the semantic content of the image and distinguishing the noise or artifacts. A third aspect that will affect the perception of image quality is the image's appearance characteristics such as brightness, contrast, sharpness, and colorfulness. A bright image and a dark image will be perceived as having different quality even if the semantic content and the distortion are the same. Similarly the same image displayed in colour and in gray-scale will have different perceived qualities. Therefore, a combination of at least three factors, semantic content, distortion and appearance, will affect the perceived visual quality of the image.

Therefore, the challenge of developing BIQA models is how to encode the **semantic content, distortion and appearance**



Fig. 1. Example images containing synthetic (a) (b) and real (c) (d) distortions. Optimal when zoomed in.

appropriately and relate them to the final perceived image quality. In this paper, we have developed a new BIQA model termed Self-supervision and Vision-Language supervision Image Quality Evaluator (SLIQUE) which models the semantic content, distortion and appearance together to assess an image’s visual quality. To enable the development of SLIQUE, we contribute a large Text Annotated Distortion, Appearance and Content (TADAC) image database. The TADAC database is the first of its kind specifically designed to exploit vision-language modeling for IQA research. The key contributions of this paper are as follows:

- We present the Self-supervision and Vision-Language supervision Image Quality Evaluator (SLIQUE) which models the image semantic contents, distortions and appearances together to assess the visual quality of images. SLIQUE exploits vision-language modeling and self-supervised deep learning to distill high level knowledge about the image semantic contents, distortion characteristics and appearance properties together in the BIQA model to provide accurate and reliable assessment of the visual quality of images.
- We have developed a systematic method for constructing large text annotated image databases designed for exploiting vision-language modeling for image quality assessment and present the Text Annotated Distortion, Appearance and Content (TADAC) database containing over 1.6 million images annotated with texts about their semantic contents, distortion characteristics and appearance properties. We used existing labels or automatic image captioning to annotate the semantic content, designed a list of suitable textual phrases for describing the distortion characteristics, and developed automatic algorithms for computing the appearance properties and annotated these properties with suitable textual descriptions. The TADAC database is the first of its kind that is annotated with all three types of quality relevant texts to enable the learning of high level knowledge about all possible factors affecting image quality. TADAC has enabled the development of the first BIQA model (SLIQUE) that jointly models semantic content, distortion and appearance. We will make TADAC publicly available.

II. RELATED WORK

A. Blind Image Quality Assessment

Traditional BIQA methods mainly focus on designing hand-crafted features as the representation to predict the quality scores. Among them, models based on natural scene statistics (NSS) are widely studied, such as NIQE [25]. Another kind of techniques is based on visual codebooks.

Recently, the success of many deep learning-based computer vision tasks has inspired a number of BIQA models based on deep networks. However, lacking large labeled training dataset is one of the major challenges. One of the strategies is to use various approaches to augment the training datasets. PaQ-2-PiQ [49] introduces a large IQA dataset that includes images and patches to train IQA models. MUSIQ [17] uses multi-scale data for training. The model in [2] predicts the overall quality score of the image by combining scores of image patches, and the model in [62] adopts meta-learning to achieve the training. The DB-CNN model [52] uses synthetic and authentic distortion images to finetune a dual-stream pretrained network. The staircase structure model in [40] integrates feature from intermediate layers into final feature representation through mixed database training strategy. The model in [43] implements graph attention network to aggregate features decomposed by fully-connected layers. The model in [54] have developed a multi-task learning method where they apply language-supervised multi-task learning to assess image quality, recognize scenes, and identify distortions. By using textual descriptions of distorted images, they create image-text pairs to finetune the CLIP [32] model. GRPQ [38] learning low-level quality features agnostic to distortion types. Further, fine-tuning one such model to extract high-level image quality information through simple relevant text prompts.

B. Vision-Language Contrastive Learning

Vision-language contrastive learning is a mechanism that combines vision and language understanding. It learns to associate images and their textual descriptions in a shared embedding space. Through a contrastive loss function, the embedding textual vector and the visual vector of the same image are encouraged to be closer, while those of different images are pushed farther apart. Vision-language contrastive learning bridges the gap between vision and language, opening up new possibilities in image-text analysis. It is commonly used in multimodal tasks, including text-driven image manipulation [8], [47], image captioning [15], object detection [37],

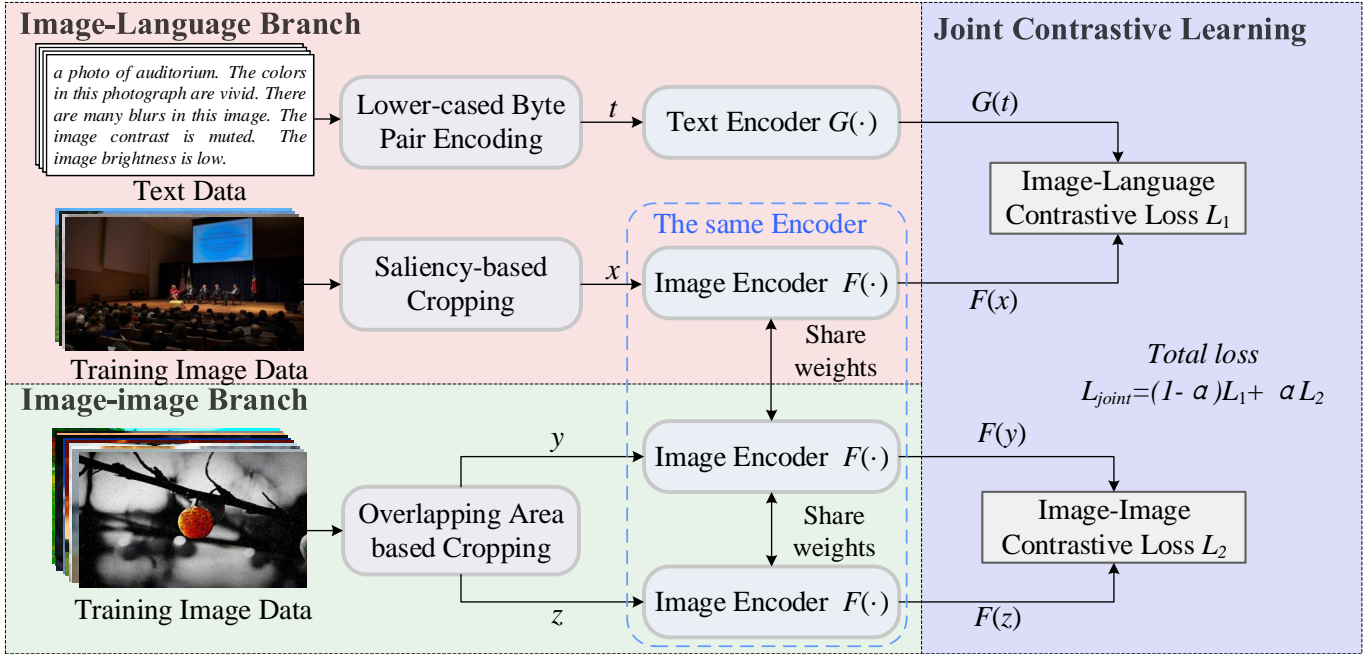


Fig. 2. Training the image encoder of SLIQUE. The Image-Language Branch performs vision-language contrastive learning for aligning text labels and image contents and the Image-Image Branch carries out self-supervised visual learning. The objective is to train the image encoder for extracting discriminative image features that capture all categories of quality relevant image attributes. Note all three image encoders in the diagram are identical triplets. The purpose of the saliency-based cropping module is to use visual saliency for cropping a high resolution sub-image containing the maximum amount of visual information during training (rather than using the whole image which can be too large). After the system is trained, only the image encoder is used for extracting image features for predicting the image quality, see Section III-B.

[56], and semantic segmentation [33], [58]. The majority of aforementioned works focus on understanding the high-level semantic of images through vision-language contrastive learning. The application of vision-language contrastive learning to learn image representations for BIQA has just started to attract the attention of researchers [44] where simple abstract textual descriptions like “good photo” and “bad photo” are used to fine-tune the pre-trained CLIP model [31]. However, as visual quality involves multiple influencing factors, it is insufficient to use simple abstract textual descriptions in providing enough textual information for image quality perception. Our method addresses the above limitations by designing and adopting text that is more diverse and related to image quality. We embed text information into the model using a language supervision contrastive learning approach, enabling SLIQUE to more accurately extract image quality features.

C. Visual Self-supervised Learning

Visual self-supervised learning is also a potential method for overcoming the problem of lacking labeled data. There are two main approaches: generative-based [12] and contrastive-based [13], [50]. In BIQA, self-supervised learning has already been utilized. SAWAR [60] applies a self-supervised generative-based learning architecture of collaborative auto-encoding, using content autoencoder and distortion autoencoder to represent content and distortion respectively. CONTRIQUE [22] employs visual contrastive learning by setting positive and negative samples through the classification of distortion type or distortion severity. Re-IQA [34] adopts a dual-stream

pre-trained network, with one stream using an ImageNet [5] to train a content encoder and the other stream using distortion dataset to train a distortion encoder. SPIQ [3] exploits a sample pairing strategy, where sub-images that are distant from each other within an image are defined as negative samples, while those that are closer are defined as positive samples. QPT-Resnet50 [55] introduces a distortion degradation space to generate a variety of complex distortion images which are used in visual contrastive learning. In this paper, we not only employ visual contrastive learning but also apply vision-language learning to provide language supervision knowledge together to predict image quality.

III. SLIQUE

Our new BIQA model is termed Self-supervision and Vision-Language supervision Image Quality Evaluator (SLIQUE) and the training of its major part, the image encoder is shown in Fig. 2. The design of the SLIQUE architecture and training algorithm addresses the major challenges in BIQA as discussed previously. First, it employs self-supervised learning to exploit large amount of readily available unlabeled images. Second, it uses language-vision contrastive learning to embed high level quality relevant knowledge into the BIQA model. Third, it constructs a large Text Annotated Distortion, Appearance and Content (TADAC) image database for training the SLIQUE such that it can acquire quality relevant high level knowledge to accurately predict the visual quality of images.

A. Joint Contrastive Learning

The SLIQUE architecture in Fig. 2 has an image-language branch and an image-image branch, and each of the two branches has a two-stream architecture to achieve the joint contrastive learning.

Image-language branch: This branch consists of a language encoder G and an image encoder F . The encoder G transforms the input textual description t to an embedding feature $G(t)$. Similarly, F transforms the input image x to a feature $F(x)$. Note that $G(t)$ and $F(x)$ have the same dimension by design so that the similarity between them can be readily calculated. The training objective of the image-language branch is to match images with their textual labels which contain descriptions of image content, distortion and appearance information. Specifically, the InfoNCE loss [29] is employed to constrain the image-language branch:

$$l = -\log \frac{\exp(q \cdot k_+ / \tau)}{\sum_{i=0}^N \exp(q \cdot k_i / \tau)} \quad (1)$$

where q is an encoded query, k_i is the i -th encoded key of a dictionary consisting of N samples, and k_+ is a single key that matches q . And τ is a temperature hyper-parameter.

$$L_1 = \sum_i l \left(\dots, F(x_n^i), G(t_n^i), \dots \mid \langle x_n^i, t_n^i \rangle \in \mathcal{B}_i, \right. \\ \left. 1 \leq n \leq N \right) \quad (2)$$

where $l(\cdot)$ is defined in Equation (1), \mathcal{B}_i denotes the i -th training batch consisting of 1 positive sample pair and $N-1$ negative sample pairs, and $\langle x_n^i, t_n^i \rangle$ is the n -th ($1 \leq n \leq N$) sample pair of image-language in \mathcal{B}_i . The pairing strategy can be found in Section III-D. Based on Equation (2), the image-language branch should be able to capture the intrinsic correlation between visual and textual representations.

Before sending the input text to the language encoder, we represent it by the lower-cased byte pair encoding (BPE). Another common practice is resizing the input image to a fixed size. However, the resizing operation generally alters the perceptual quality of images. Thus, during training the encoders in Fig. 2, we crop a sub-image from the input image instead of resizing. Cropping is based on the visual saliency of the input. Specifically, a saliency map is first predicted from the input image by hierarchical knowledge embedding [59]. Subsequently, a sub-image with a fixed size is cropped at the position where the sum of saliency values within the sub-image is the maximum. As will be shown in ‘‘Implementation Details’’ part of Section IV, during the training phase of joint contrastive learning, the cropped sub-image covers a considerable part of the input image. Thus, it is reasonable to assume that the image information are well preserved in the cropped images.

Image-image branch: This branch is similar to the above image-language branch. The main difference is that no language encoder is required here. Instead, two input images y and z are transformed concurrently by the image encoder F into a feature space. The two image encoders in this branch

are a pair of identical twins which is exactly the same as the image encoder in the image-language branch. In other words, the three ‘‘Image Encoder’’ modules illustrated in Fig. 2 are identical triplets and share the same parameters all the time. This design is important, since it ensures the output features from the two branches are in the same embedding space.

Another difference is that training samples prepared for this branch are image-image pairs rather than image-language ones. Thus, the constraint on the image-image branch can be expressed as Equation (3).

$$L_2 = \sum_j l \left(\dots, F(y_m^j), F(z_m^j), \dots \mid \langle y_m^j, z_m^j \rangle \in \mathcal{A}_j, \right. \\ \left. 1 \leq m \leq M \right) \quad (3)$$

where \mathcal{A}_j denotes the j -th training batch consisting of 1 positive sample pair and $M-1$ negative sample pairs and $\langle y_m^j, z_m^j \rangle$ is the m -th ($1 \leq m \leq M$) sample pair of image-image in \mathcal{A}_j . Here we adopt the overlapping area (OLA) based cropping [34] to ensure that two sub-images in a positive sample pair are with similar quality. Details of the pairing strategy can be found in Section III-D.

Joint training: To determine the learnable parameters in the encoders G and F , we do not directly employ or fine-tune publicly released models [27] that have already been trained for other tasks. Instead, we jointly optimize the two branches from scratch based on contrastive learning:

$$L_{joint} = (1 - \alpha)L_1 + \alpha L_2 \quad (4)$$

where α is the parameter to balance the image-image branch and the image-language branch. After minimizing Equation (4), the encoder parameters are frozen. The image encoder F is used to extract image features which are then fed to a simple regression neural network to predict the image quality.

B. Regression to Quality Score

Similar to [1] [22], we use a simple ridge regression to map image features to a visual quality score. The regression is supervised by the Mean Opinion Score (MOS) from IQA datasets based on the L_1 loss. Note that given an image to be assessed, its textual description may be not comprehensive or even not available at all in real-world scenarios. Thus, the language encoder is excluded in the regression, and we do not require the textual description of an image to achieve the quality assessment in the testing.

C. Construction of database

In order to train the joint contrastive representation learning module, we have constructed a large Text Annotated Distortion, Appearance and Content (TADAC) image database. Each image in TADAC is annotated with three types of textual descriptions indicating the semantic contents, the distortion characteristics and the appearance properties respectively.

Image Data Preparation: Images with diverse contents and various distortions are required to train the joint contrastive learning framework. The data should not be biased towards

a particular type of image quality, thereby avoiding potential shortcomings in generalization performance. Thus, we collect images with both synthetic distortions and authentic distortions from multiple image databases. Notably, no MOS annotation is required for the collected images.

For synthetic distortions, we include 700,000 distorted images from the KADIS dataset [20], which contains 25 distortion types and each type has 5 levels of severity. Besides, the 140,000 pristine images from this dataset are also included, resulting in a total of 840,000 images. Although these images have no MOS annotations, they have already been annotated by semantic labels (scene and object) and distortion labels (type and level).

In addition to synthetic distortion images, we collected 809,850 images with authentic (real) distortion from five datasets: 255,000 from AVA [28], 120,000 from COCO [21] training set, 33,000 from VOC [6], 400,000 from Places365 [57], and 1,850 from CERTH-Blur [23]. These datasets were originally built for various other purposes, e.g., the VOC database is introduced for the object recognition task. Thus, the labels for these images are also diverse. In brief, the images collected from CERTH-Blur are without any kinds of labels while the remaining images have scene category labels. The total number of category for these images is 26,332.

Content, Distortion and Appearance Annotation Texts: After collecting more than 1.6 million images, we need to prepare textual descriptions for them. As the joint contrastive learning is designed for the BIQA, the textual descriptions should be highly related to visual quality of images. It has been demonstrated that the visual quality of an image depends on its content, its distortion, and the interaction between them [60]. Thus, the annotation texts should describe the images content, distortion and their appearance characteristics.

For image content description text, we adopt the textual template format of “A photo of a(n) $\{s\}$ ”, where $\{s\}$ is given by the scene label or object label of the image. This template allows us to summarize the overall content information of the image based on $\{s\}$. Fortunately, most images collected above contain scene or object labels. For the images without semantic labels, we obtain their content description texts by employing the image captioning method in [26].

For the images containing synthetic distortions, we annotate them with their distortion labels. We observe that some distortion types give rise to very similar visual appearances, such as Gaussian blur and lens blur. Thus, when preparing textual descriptions of synthetic distortions, due to the similarity of the languages in the visual senses, we combine the 25 distortion types from the KADIS dataset into 19 types (details in Appendix A in the supplementary materials). Thus, there are a total of 95 kinds of distortion (19 types \times 5 degrees). For each of these 19 distortion types, we design a set of 10 possible descriptive phrases for it (see Appendix A in the supplementary materials). For each of the 5 degrees of distortion, we design a list of adjectives, adverbs, and quantifiers for it as well (see Appendix A in the supplementary materials). To annotate the images with synthetic distortions, we designed one list of phrases describing distortion types and another list of adjectives, adverbs, and quantifiers describing

the degree of distortions. To annotate an image, we randomly select a phrase from the list corresponding to the distortion type and choose another from the list corresponding to the degree of distortion.

For example, for a given image that contains “blur” distortion with a degree of 3, the textual description will be one of the phrases randomly picked from the 10 phrases describing “blur”. The adjectives, adverbs or quantifier in that phrase will be randomly picked from the list corresponding to degree 3. The annotation text for this image may be “some blurring”. It is clear that for the same image, there are many equivalent annotations.

For the 140,000 pristine images with high quality, we design another text set consisting of 20 descriptive phrases (see Appendix A in the supplementary materials). These phrases are used to capture possible ways of describing images with high quality. For any one of these images, a phrase randomly picked from these 20 is assigned as its annotation. Note that one image can be assigned multiple annotations.

For images containing authentic (real) distortions, they are much harder to describe textually because they may contain complex and multiple distortions. As the distortions are unknown, our approach is to annotate these images by their appearance characteristics based on 4 quality relevant aspects: brightness, contrast, sharpness, and colorfulness [11], [42]. For a given image, we first calculate its brightness (BR), contrast (CT), sharpness (SH), and colorfulness (CL) (detailed procedures for calculating these are described in Appendix B in the supplementary materials). We then classify these BR, CT, SH and CL values as “high”, “medium” and “low” categories based on their value distributions. For each value category within every aspect, we design 20 suitable descriptive phrases. In total we have $4 \times 3 \times 20 = 2400$ phrases for annotating images containing real distortions (see Appendix B in the supplementary material). For a given image, we label each aspect with a phrase randomly picked from the list corresponding to its value category. For example, for an image whose CT has a “medium” value, we randomly pick one of the 20 phrases corresponding to medium CT value. Note that in the current version of the TADAC dataset, these appearance descriptions were assigned to the subset of images containing real distortions, they can be easily applied to the whole database.

Based on the above procedures, we have constructed a database containing images of diverse contents, a variety of distortions and rich appearances. Importantly, these images are annotated with texts describing their semantic contents, distortion characteristics and appearance properties. These texts can represent quality relevant high level knowledge. When used to train the joint contrastive representation learning framework in Fig. 2, they should enable the system to capture these quality relevant knowledge in its representation vectors. Obviously, the database can be used in other contexts and will be particularly useful for developing IQA applications.

D. Training Sample Pairing Strategy

It is required to produce positive and negative sample pairs for both the vision-language and the visual contrastive

TABLE I
PERFORMANCE COMPARISONS OF SLIQUE AGAINST VARIOUS BIQA MODELS ON IQA DATABASES WITH SYNTHETIC DISTORTIONS. HIGHER SROCC AND PLCC IMPLY BETTER PERFORMANCE. THE ENTRY MARKED AS ‘-’ MEANS THE RESULTS ARE UNAVAILABLE.

Method	LIVE		CSIQ		TID2013		KADID		Weighted Average	
	SROCC \uparrow	PLCC \uparrow	SROCC \uparrow	PLCC \uparrow	SROCC \uparrow	PLCC \uparrow	SROCC \uparrow	PLCC \uparrow	SROCC \uparrow	PLCC \uparrow
BRISQUE	0.939	0.935	0.746	0.829	0.604	0.694	0.528	0.567	0.580	0.629
NIQE	0.907	0.901	0.627	0.712	0.315	0.393	0.374	0.428	0.408	0.464
CORNIA	0.947	0.950	0.678	0.776	0.678	0.768	0.516	0.558	0.583	0.636
DB-CNN	0.968	0.971	0.946	0.959	0.816	0.865	0.851	0.856	0.855	0.870
WaDIQaM	0.955	0.960	0.852	0.844	0.835	0.855	0.739	0.752	0.777	0.790
PQR	0.965	0.971	0.872	0.901	0.740	0.798	-	-	-	-
P2P-BM	0.959	0.958	0.899	0.902	0.862	0.856	0.840	0.849	0.854	0.859
HyperIQA	0.962	0.966	0.942	0.955	0.840	0.858	0.852	0.845	0.860	0.860
MetalQA	0.960	0.959	0.899	0.902	0.856	0.868	0.853	0.846	0.862	0.860
MUSIQ	0.837	0.818	0.697	0.766	-	-	0.572	0.584	-	-
UNIQUE	0.969	0.968	0.902	0.927	-	-	0.878	0.876	-	-
CONTRIQUE	0.960	0.961	0.947	0.958	0.861	0.871	0.934	0.937	0.921	0.925
Re-IQA	0.970	0.971	0.947	0.960	0.804	0.861	0.872	0.885	0.867	0.889
SAWAR	0.973	0.978	0.961	0.967	0.884	0.896	0.928	0.930	0.923	0.927
CLIP-IQA+	0.948	0.952	0.907	0.928	0.835	0.857	0.913	0.909	0.898	0.901
GRepQ	0.953	0.958	0.941	0.950	-	-	-	-	-	-
SLIQUE	0.982	0.982	0.966	0.973	0.884	0.899	0.957	0.959	0.943	0.948

learning. Clearly, the pairing strategy should be appropriate for the BIQA task. The optimization objective of image-language branch is to judge whether the input text corresponds to the visual quality of the input image. Thus, an image-language pair is a positive one if the text comes from the descriptions of the content, distortion or appearance of the image. Otherwise, the pair is a negative one. For the image-image branch, we follow the same pairing scheme as in [34], where two sub-images cropped from an image with 10% to 30% overlapping are treated as a positive pair, and two sub-images cropped from different images form a negative pair.

E. Comparisons with Previous BIQA Works

As far we are aware, SLIQUE is the first BIQA model that explicitly models all three types visual quality relevant attributes, semantic contents, distortion characteristics and appearance properties. Our method is joint contrastive learning which combines vision-language supervised contrastive learning and visual self-supervised contrastive learning, and can take full advantage of these two contrastive learning methods. With the joint contrastive learning mechanism, our model is distinguished from the models that only use a vision-language supervised contrast learning mechanism (such as CLIP-IQA [44] and LIQE [54]), as well as the models with only visual self-supervised contrast learning (such as CONTRIQUE and Re-IQA). Removing either contrastive learning degrades the performance of the model as will be detailed in the ablation study of Table IV. Furthermore, we have constructed the first of a kind database specifically designed for learning all three categories of quality bearing image features. We have developed a systematic approaches to constructing quality relevant image textual labels for exploiting vision-language modeling technology to advance research in IQA.

IV. EXPERIMENTS

A. Implementation Details

The implementation is based on PyTorch and a machine with 8 Nvidia A100-40GB GPUs. In the joint contrastive learning architecture, we employ ResNet-50 followed by an adaptive pooling layer and 2 multilayer perceptron (MLP) layers as the image encoder F . The language encoder G is implemented as GPT-2 with 63M parameters², which uses the byte-pair encoding with a vocabulary size of 49K tokens and a maximum context length of 77. The output features of both the image and the language encoders have a size of 512×1 . Most collected images used in the joint contrastive learning have a size of 512×384 ³, and all the cropped sub-images (either the saliency based or the OLA based) have a size of 224×224 . The collected image data is also augmented in the same manner as [22]. The temperature parameter in the InfoNCE loss is set to 0.1 by following the suggestion in [29]. The default value of α in Equation (4) is 0.7, which will be discussed in Ablation Studies. The SGD optimizer with initial learning rate of 0.006 and batch size of 1024 is used to train the network of joint contrastive learning. Furthermore, the learning rate undergoes a linear warm-up for the first two epochs and then follows a cosine decay schedule without restarts. The training starts from scratch and stops when the epoch number reaches 30.

The ridge regression is learned on some IQA dataset with images labeled with MOS. We include 8 datasets in the experiments, including LIVE [36], CSIQ [18], TID2013 [30], and KADID [19], KonIQ [16], CLIVE [9], FLIVE [49], and SPAQ [7]. Among these datasets, the first four are based on synthetic

²We are aware there exist newer and more powerful large language models (LLMs). Although a more powerful model could well lead to better results, the goal here is to demonstrate the technical soundness of the designing principle of SLIQUE.

³Some authentic distortion images are slightly larger than 512×384 . We simply resize them to 512×384 .

TABLE II
PERFORMANCE COMPARISONS OF SLIQUE AGAINST VARIOUS BIQA MODELS ON IQA DATABASES WITH AUTHENTIC DISTORTIONS.

Method	KonIQ		CLIVE		FLIVE		SPAQ		Weighted Average	
	SROCC \uparrow	PLCC \uparrow	SROCC \uparrow	PLCC \uparrow	SROCC \uparrow	PLCC \uparrow	SROCC \uparrow	PLCC \uparrow	SROCC \uparrow	PLCC \uparrow
BRISQUE	0.665	0.681	0.608	0.629	0.288	0.373	0.809	0.817	0.342	0.419
NIQE	0.531	0.538	0.455	0.483	0.211	0.288	0.700	0.709	0.260	0.329
CORNIA	0.780	0.795	0.629	0.671	0.311	0.356	0.709	0.725	0.363	0.405
DB-CNN	0.875	0.884	0.851	0.869	0.435	0.652	0.911	0.915	0.491	0.682
WaDIQaM	0.797	0.805	0.671	0.680	0.571	0.430	0.840	0.845	0.600	0.477
PQR	0.880	0.884	0.857	0.882	-	-	-	-	-	-
P2P-BM	0.872	0.885	0.844	0.842	0.535	0.623	0.847	0.830	0.574	0.651
HyperIQA	0.906	0.917	0.859	0.882	0.554	0.623	0.916	0.919	0.597	0.659
MetaIQA	0.850	0.887	0.802	0.835	0.540	0.507	0.822	0.804	0.576	0.548
MUSIQ	0.916	0.928	0.828	0.785	0.646	0.739	0.917	0.921	0.678	0.760
UNIQUE	0.896	0.910	0.854	0.890	-	-	-	-	-	-
CONTRIQUE	0.896	0.901	0.845	0.857	0.580	0.641	0.914	0.919	0.619	0.674
Re-IQA	0.914	0.923	0.840	0.854	0.645	0.733	0.918	0.925	0.677	0.756
SAWAR	0.894	0.906	0.846	0.857	0.544	0.642	0.916	0.919	0.588	0.674
CLIP-IQA+	0.895	0.909	0.805	0.832	0.540	0.566	0.864	0.866	0.581	0.605
GRepQ	0.855	0.861	0.822	0.836	-	-	-	-	-	-
SLIQUE	0.916	0.929	0.897	0.901	0.720	0.754	0.921	0.925	0.744	0.775

distortions while the last four are built for authentic distortions. The images in SPAQ are resized such that the shorter side is 512 by following the suggestion in [7], while the image sizes in other datasets remain unchanged. In each dataset, three sets are randomly splitted for learning, validation, and testing respectively. For the FLIVE dataset, we follow the splitting scheme recommended by its authors. For the other 7 datasets, 70% of the data are used for learning, 10% are the validation set, and the remaining are used for testing. As the learning of ridge regression requires no iteration, we use the validation set to determine the regularization coefficient in the regression. The random splitting is repeated 10 times, and the mean results of the testing set are recorded to avoid possible bias. The above protocols of image resizing and dataset splitting have been adopted in many recent IQA researches [22], [34], [60]. Thus, we follow the same protocols to make the following comparisons fair.

B. Results and Comparisons

We test our model on the above mentioned 8 IQA datasets and compare it with 15 BIQA models. The competitors include 16 BIQA methods: BRISQUE [24], NIQE [25], CORNIA [48], WaDIQaM [2], PQR [51], DB-CNN [52], P2P-BM [49], HyperIQA [39], MetaIQA [62], MUSIQ [17], UNIQUE [53], CONTRIQUE [22], Re-IQA [34], SAWAR [60], CLIP-IQA [44], and GRepQ [38]. All results of BIQA are either from the original papers or reproduced by their source codes.

Two widely-used criteria Spearman rank-order correlation coefficient (SROCC) and the Pearson linear correlation coefficient (PLCC) are used to measure the performance of different BIQA models. Table I and Table II list the quantitative results on synthetic distortion datasets and authentic distortion datasets, respectively. The best and second-best results are highlighted in bold. The proposed method achieves 16 best results across all IQA datasets. It indicates that our

model exhibits excellent performances on both synthetic and authentic distortions. We attribute it to the data preparation of both synthetic distortion and authentic images for the joint contrast learning. In contrast, only synthetic distortion images can be employed to train the auto-encoders of SAWAR in a self-supervised way. Thus, the performance of SAWAR on authentic distortion datasets is inferior, although its performance on synthetic distortion datasets is impressive. In the CONTRIQUE and Re-IQA models, both types of distortions can be employed to train the quality-relevant feature extractors. However, they only consider visual contrast learning and ignore the benefits of language supervised learning. In addition, the CLIP-IQA model is mainly devoted to exploit the knowledge already contained in the pre-trained CLIP and finetune with simple statements. Different from them, the proposed method based on vision-language and visual contrastive learning can achieve superior results by using a more comprehensive text description.

C. T-SNE Visualization of Quality Relevant Features

The success of SLIQUE relies on its image encoder's ability to extract discriminative image features that can capture information related to factors affecting image quality such as semantic content, distortion characteristics and appearance properties. Fig. 3 shows examples of t-SNE visualization of the learned representations of SLIQUE and that of a recent method CONTRIQUE [22]. We used 750 images sampled from CSIQ (Synthetic distortions - #600) and User-Generated Content (UGC) images from KonIQ (UGC - #150) and pristine images from KADIS (Natural images - #150). It is clearly seen that, for the CONTRIQUE model, some features from differently distorted images are not well distinguished from each other, e.g., the JPEG and the Pink noise. In contrast, the representations learned by our new SLIQUE can better separate different distortion types which may explain why it has superior performances.

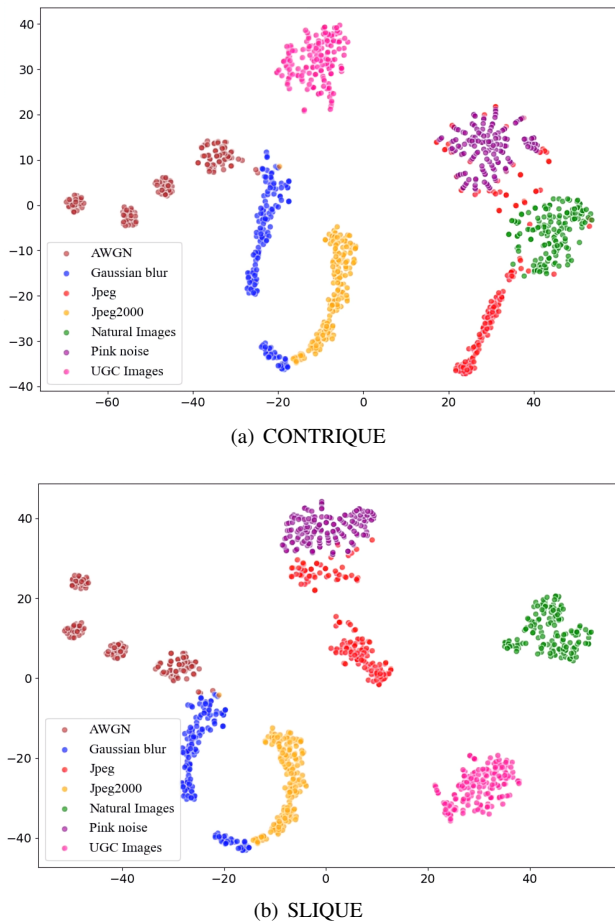


Fig. 3. 2D t-SNE visualizations of learned representations. For both CONTRIQUE and SLIQUE, we conducted 2D t-SNE visualization experiments using 7 different types of distorted images from 3 image databases.

D. Cross Dataset Evaluation

To show the generalization ability of SLIQUE, we further conduct cross dataset evaluations by training and testing on different datasets. Specifically, the ridge regression of SLIQUE is learned by all the data from a dataset while the parameters of image encoder F are still frozen. Then, the model is tested on all the data from another dataset. Four datasets, including two synthetic and two authentic distortion datasets, are involved in the cross dataset evaluation. The results based on SROCC are presented in Table III, where the performances of two recently-developed models are also listed. As shown in Table III, our model outperforms the Re-IQA and the SAWAR models, although all these three models take advantage of unsupervised learning to obtain quality-relevant features. It demonstrates that our joint contrastive learning is highly effective in representing the image quality.

TABLE III
CROSS DATABASE EVALUATIONS OF IQA MODELS.

Training	Testing	Re-IQA	SAWAR	SLIQUE
LIVE	CSIQ	0.808	0.898	0.903
CSIQ	LIVE	0.929	0.930	0.934
CLIVE	KonIQ	0.769	0.665	0.775
KonIQ	CLIVE	0.794	0.700	0.832

E. Ablation Studies

Four datasets, i.e., CSIQ, KADID, KonIQ and CLIVE, are used in the ablation studies to investigate the effectiveness of some important designs and settings in SLIQUE. We have conducted 6 ablation studies, including the discussions on individual contrastive learning, the value of parameter α , the starting point of optimization, annotation texts, different sizes of training data, and the usage of language feature.

Individual contrastive learning. We first conducted an ablation study to validate the importance of joint contrastive learning by disabling one of the branches. When disabling the image-image branch, only image-language pairs are used to train the encoders G and F from scratch. Similarly, if the image-language branch is disabled, only image-image pairs are employed to train the image encoder F . The results based on SROCC are given in Table IV, which shows a performance reduction if we disable either branch. Moreover, we can see from the results that the visual contrastive learning is greatly important, and the vision-language contrastive learning also provides essential benefits.

TABLE IV
PERFORMANCE OF INDIVIDUAL CONTRASTIVE LEARNING.

Ablation cases	CSIQ	KADID	KonIQ	CLIVE
w/o Image-Image	0.877	0.849	0.787	0.673
w/o Image-Language	0.949	0.933	0.897	0.847
SLIQUE	0.966	0.957	0.916	0.897

Value of parameter α . The parameter α is used to balance the contributions of the image-image branch and the image-language branch. We set a range of α values from 0.6 to 0.8 with a step size of 0.01 to test SLIQUE. The SROCC-based performance is shown in Fig. 4, where we can see that the model performance is stable and can reach the maximum within the interval of $[0.65, 0.75]$. Thus, it is reasonable to set the default value of α to 0.7. This value further demonstrates the importance of visual learning as well as the necessity of vision-language learning.

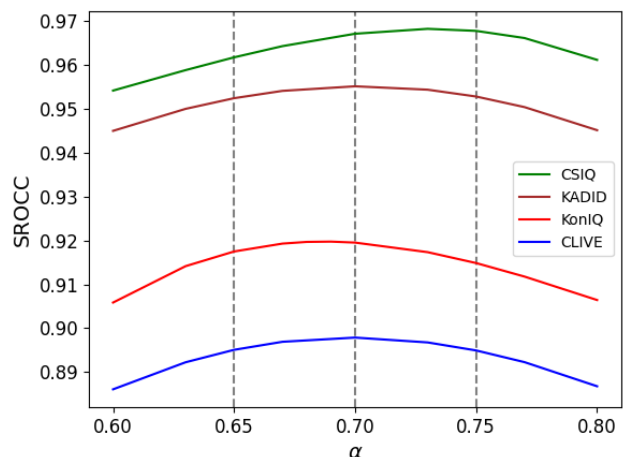


Fig. 4. Impact of parameter α on the model performance.

Starting point of optimization. In the joint training of image-language branch and image-image branch, we optimize the language encoder G and the image encoder F from scratch. An alternative strategy is to optimize them (or one of them) from pre-trained models. Here we employed two well-known pre-trained models, i.e., CLIP and SIMCLR, as the starting point of optimization. The results on synthetic distortion datasets and authentic distortion datasets are recorded in Table V and Table VI, respectively. In the first row of each table, the language encoder G is initialized by the pretrained CLIP weights, and the image encoder F is initialized by the pretrained SIMCLR weights. Other cases are included in the following rows. As the SIMCLR only contains image encoder, it can not used to initialize G . From the results in Table V and Table VI, we find that the optimizations from pretrained models do not result in the best performances, although some performances from them are comparable with state of the art. It may be because that they are originally trained in object recognition or image classification tasks. Thus, using pretrained models is not optimal for the image quality assessment task.

TABLE V
OPTIMIZATION FROM PRETRAINED MODELS VERSUS FROM SCRATCH
(SYNTHETIC DISTORTION DATASETS).

Language encoder	Image encoder	CSIQ	KADID
from CLIP	from SIMCLR	0.886	0.875
from CLIP	from CLIP	0.912	0.907
from CLIP	from scratch	0.932	0.928
from scratch	from CLIP	0.926	0.918
from scratch	from SIMCLR	0.945	0.936
SLIQUE (both from scratch)		0.966	0.957

TABLE VI
OPTIMIZATION FROM PRETRAINED MODELS VERSUS FROM SCRATCH
(AUTHENTIC DISTORTION DATASETS).

Language encoder	Image encoder	KonIQ	CLIVE
from CLIP	from SIMCLR	0.866	0.839
from CLIP	from CLIP	0.809	0.741
from CLIP	from scratch	0.909	0.879
from scratch	from CLIP	0.884	0.765
from scratch	from SIMCLR	0.878	0.838
SLIQUE (both from scratch)		0.916	0.897

Components in annotation texts. To investigate the impact of different components in the annotation texts on quality prediction, we conducted ablation studies by excluding some components in the textual descriptions, resulting in 4 cases. The results based on SROCC are shown in Table VII. In the first row of Table VII, we only keep the content annotation texts, and exclude both the distortion texts for synthetic distortion images and the appearance texts for authentic distortion images. The results in the first, second, and third rows respectively indicate that using only content text, distortion text, or appearance attribute text alone is insufficient. In the fourth row, we add the distortion information of synthetic distortion images to the textual descriptions. The results show

that the performance on authentic distortion datasets KonIQ and CLIVE even decreases, although the performance on synthetic distortion datasets is improved. It may be attributed to the large differences between the synthetic distortion and the authentic distortion. Similarly, the results of adding the appearance texts are provided in the fifth row which is worse than the full model. In the sixth row, we report the results of excluding content texts, demonstrating that the content texts are also beneficial to the IQA task.

TABLE VII
ABLATION STUDIES ON COMPONENTS IN ANNOTATION TEXTS. IN EACH COLUMN, THE TOP PERFORMANCE IS BOLDFACED.

Annotation texts	CSIQ	KADID	KonIQ	CLIVE
Content	0.944	0.942	0.901	0.884
Distortion	0.948	0.944	0.885	0.872
Appearance	0.931	0.938	0.904	0.888
Content+Distortion	0.962	0.952	0.891	0.879
Content+Appearance	0.950	0.946	0.914	0.894
Distort.+Appearance	0.963	0.953	0.909	0.890
Full Texts (SLIQUE)	0.966	0.957	0.916	0.897

The amount of training. To investigate the impact of the amount of training data, we divided the TADAC database into equal proportions of 20%, 40%, 60%, 80%, and 90%. We can observe from the results in Table VIII that using a large number of data is essential in training our two branches. Besides, the results reveal that our method can achieve state-of-the-art performance by using 90% of the data.

TABLE VIII
SROCC PERFORMANCES OF OUR MODEL FOR DIFFERENT AMOUNT OF TRAINING DATA.

Datasets proportion	CSIQ	KADID	KonIQ	CLIVE
20%	0.909	0.910	0.875	0.813
40%	0.932	0.935	0.889	0.834
60%	0.946	0.941	0.903	0.866
80%	0.953	0.949	0.913	0.888
90%	0.966	0.957	0.917	0.897

Usage of language feature. In our SLIQUE, only the image feature is employed in the prediction of visual quality of images. An alternative strategy is to use an image captioning method to produce a textual description for the image to be accessed. With such a strategy, the feature from language encoder can also be fed to the ridge regression. Here we employed the captioning method in [26] to produce annotation texts. The results on synthetic distortion datasets and authentic distortion datasets are recorded in Table IX and Table X, respectively. From the results, we can see that using the language feature is not helpful. It is mainly because the texts produced from the captioning method contain little distortion and appearance information. Furthermore, even if the captioning method can produce perfect texts for the IQA task, the language feature would be redundant due to its similarity to the corresponding image feature.

V. CONCLUDING REMARKS

We reasoned that the semantic contents, the distortions characteristics, and the appearance properties all affect the

TABLE IX

EXPLORING MORE FEATURES TO USE IN EVALUATION OF SYNTHETIC DISTORTION DATASETS.

Feature for evaluation	CSIQ	KADID
Language feature + Image feature	0.941	0.939
SLIQUE (only image feature)	0.966	0.957

TABLE X

EXPLORING MORE FEATURES USED IN THE EVALUATION OF AUTHENTIC DISTORTION DATASETS.

Feature for evaluation	KoniQ	CLIVE
Language feature + Image feature	0.899	0.861
SLIQUE (only image feature)	0.916	0.897

perceived image quality. Recognizing one of the most challenging problems in Image Quality Assessment (IQA) is that these intertwining factors confound a solution, we have developed a new blind image quality assessment (BIQA) model that exploits vision-language supervised modeling and visual self-supervised learning to acquire all these quality relevant representation features together. We have shown that our Self-supervised and Vision-Language supervised Image Quality Evaluator (SLIQUE), the first BIQA model that jointly models image semantic contents, distortions and appearances together and trained based on the newly constructed large Text Annotated Distortion, Appearance and Content (TADAC) image database, is capable of achieving superior performances to state of the art BIQA models, demonstrating the soundness of SLIQUE’s design principles and the effectiveness of its implementation.

REFERENCES

- [1] Philip Bachman, R Devon Hjelm, and William Buchwalter. Learning representations by maximizing mutual information across views. *Advances in Neural Information Processing Systems*, 32, 2019.
- [2] Sebastian Bosse, Dominique Maniry, Klaus-Robert Müller, Thomas Wiegand, and Wojciech Samek. Deep neural networks for no-reference and full-reference image quality assessment. *IEEE Transactions on Image Processing*, 27(1):206–219, 2018.
- [3] Pengfei Chen, Leida Li, Qingbo Wu, and Jinjian Wu. Spiq: A self-supervised pre-trained model for image quality assessment. *IEEE Signal Processing Letters*, 29:513–517, 2022.
- [4] Ting Chen, Simon Kornblith, Mohammad Norouzi, and Geoffrey Hinton. A simple framework for contrastive learning of visual representations. In *International Conference on Machine Learning*, pages 1597–1607. PMLR, 2020.
- [5] Jia Deng, Wei Dong, Richard Socher, Li-Jia Li, Kai Li, and Li Fei-Fei. Imagenet: A large-scale hierarchical image database. In *Proceedings of the IEEE/CVF Conference on Computer Vision and Pattern Recognition*, pages 248–255, 2009.
- [6] Mark Everingham, Luc Van Gool, Christopher KI Williams, John Winn, and Andrew Zisserman. The pascal visual object classes (voc) challenge. *International Journal of Computer Vision*, 88:303–338, 2010.
- [7] Yuming Fang, Hanwei Zhu, Yan Zeng, Kede Ma, and Zhou Wang. Perceptual quality assessment of smartphone photography. In *Proceedings of the IEEE/CVF Conference on Computer Vision and Pattern Recognition*, pages 3677–3686, 2020.
- [8] Aviv Gabbay, Niv Cohen, and Yedid Hoshen. An image is worth more than a thousand words: Towards disentanglement in the wild. *Advances in Neural Information Processing Systems*, 34:9216–9228, 2021.
- [9] Deepti Ghadiyaram and Alan C Bovik. Massive online crowdsourced study of subjective and objective picture quality. *IEEE Transactions on Image Processing*, 25(1):372–387, 2015.
- [10] S Alireza Golestaneh, Saba Dadsetan, and Kris M Kitani. No-reference image quality assessment via transformers, relative ranking, and self-consistency. In *Proceedings of the IEEE/CVF Winter Conference on Applications of Computer Vision*, pages 1220–1230, 2022.
- [11] David Hasler and Sabine E. Suesstrunk. Measuring colorfulness in natural images. In Bernice E. Rogowitz and Thrasyvoulos N. Pappas, editors, *Human Vision and Electronic Imaging VIII*, volume 5007, pages 87 – 95. International Society for Optics and Photonics, SPIE, 2003.
- [12] Kaiming He, Xinlei Chen, Saining Xie, Yanghao Li, Piotr Dollár, and Ross Girshick. Masked autoencoders are scalable vision learners. In *Proceedings of the IEEE/CVF Conference on Computer Vision and Pattern Recognition*, 2022.
- [13] Kaiming He, Haoqi Fan, Yuxin Wu, Saining Xie, and Ross Girshick. Momentum contrast for unsupervised visual representation learning. In *Proceedings of the IEEE/CVF Conference on Computer Vision and Pattern Recognition*, pages 9729–9738, 2020.
- [14] Kaiming He, Xiangyu Zhang, Shaoqing Ren, and Jian Sun. Deep residual learning for image recognition. In *Proceedings of the IEEE/CVF Conference on Computer Vision and Pattern Recognition*, pages 770–778, 2016.
- [15] Jack Hessel, Ari Holtzman, Maxwell Forbes, Ronan Le Bras, and Yejin Choi. Clipscore: A reference-free evaluation metric for image captioning. *arXiv preprint arXiv:2104.08718*, 2021.
- [16] Vlad Hosu, Hanhe Lin, Tamas Sziranyi, and Dietmar Saupe. Koniq-10k: An ecologically valid database for deep learning of blind image quality assessment. *IEEE Transactions on Image Processing*, 29:4041–4056, 2020.
- [17] Junjie Ke, Qifei Wang, Yilin Wang, Peyman Milanfar, and Feng Yang. Musiq: Multi-scale image quality transformer. In *Proceedings of the IEEE/CVF International Conference on Computer Vision*, pages 5148–5157, 2021.
- [18] Eric C Larson and Damon M Chandler. Most apparent distortion: full-reference image quality assessment and the role of strategy. *Journal of Electronic Imaging*, 19(1):011006–011006, 2010.
- [19] Hanhe Lin, Vlad Hosu, and Dietmar Saupe. Kadid-10k: A large-scale artificially distorted iqa database. In *2019 Eleventh International Conference on Quality of Multimedia Experience (QoMEX)*, pages 1–3. IEEE, 2019.
- [20] Hanhe Lin, Vlad Hosu, and Dietmar Saupe. Deepfl-iqa: Weak supervision for deep iqa feature learning. *arXiv preprint arXiv:2001.08113*, 2020.
- [21] Tsung-Yi Lin, Michael Maire, Serge Belongie, James Hays, Pietro Perona, Deva Ramanan, Piotr Dollár, and C Lawrence Zitnick. Microsoft coco: Common objects in context. In *European Conference on Computer Vision*, pages 740–755. Springer, 2014.
- [22] Pavan C Madhusudana, Neil Birkbeck, Yilin Wang, Balu Adsumilli, and Alan C Bovik. Image quality assessment using contrastive learning. *IEEE Transactions on Image Processing*, 31:4149–4161, 2022.
- [23] Eftichia Mavridaki and Vasileios Mezaris. No-reference blur assessment in natural images using fourier transform and spatial pyramids. In *2014 IEEE International Conference on Image Processing (ICIP)*, pages 566–570. IEEE, 2014.
- [24] Anish Mittal, Anush Krishna Moorthy, and Alan Conrad Bovik. No-reference image quality assessment in the spatial domain. *IEEE Transactions on Image Processing*, 21(12):4695–4708, 2012.
- [25] Anish Mittal, Rajiv Soundararajan, and Alan C Bovik. Making a “completely blind” image quality analyzer. *IEEE Signal Processing Letters*, 20(3):209–212, 2012.
- [26] Ron Mokady, Amir Hertz, and Amit H Bermano. Clipcap: Clip prefix for image captioning. *arXiv preprint arXiv:2111.09734*, 2021.
- [27] Norman Mu, Alexander Kirillov, David Wagner, and Saining Xie. Slip: Self-supervision meets language-image pre-training. In *European Conference on Computer Vision*, pages 529–544. Springer, 2022.
- [28] Naila Murray, Luca Marchesotti, and Florent Perronnin. Ava: A large-scale database for aesthetic visual analysis. In *Proceedings of the IEEE/CVF Conference on Computer Vision and Pattern Recognition*, pages 2408–2415. IEEE, 2012.
- [29] Aaron van den Oord, Yazhe Li, and Oriol Vinyals. Representation learning with contrastive predictive coding. *arXiv preprint arXiv:1807.03748*, 2018.
- [30] Nikolay Ponomarenko, Lina Jin, Oleg Ieremeiev, Vladimir Lukin, Karen Egiazarian, Jaakko Astola, Benoit Vozel, Kacem Chehdi, Marco Carli, Federica Battisti, et al. Image database tid2013: Peculiarities, results and perspectives. *Signal Processing: Image Communication*, 30:57–77, 2015.
- [31] Alec Radford, Jong Wook Kim, Chris Hallacy, Aditya Ramesh, Gabriel Goh, Sandhini Agarwal, Girish Sastry, Amanda Askell, Pamela Mishkin,

- Jack Clark, et al. Learning transferable visual models from natural language supervision. In *International Conference on Machine Learning*, pages 8748–8763. PMLR, 2021.
- [32] Alec Radford, Jeffrey Wu, Rewon Child, David Luan, Dario Amodei, Ilya Sutskever, et al. Language models are unsupervised multitask learners. *OpenAI blog*, 1(8):9, 2019.
- [33] Yongming Rao, Wenliang Zhao, Guangyi Chen, Yansong Tang, Zheng Zhu, Guan Huang, Jie Zhou, and Jiwen Lu. Densclip: Language-guided dense prediction with context-aware prompting. In *Proceedings of the IEEE/CVF Conference on Computer Vision and Pattern Recognition*, pages 18082–18091, 2022.
- [34] Avinab Saha, Sandeep Mishra, and Alan C Bovik. Re-iqa: Unsupervised learning for image quality assessment in the wild. In *Proceedings of the IEEE/CVF Conference on Computer Vision and Pattern Recognition*, pages 5846–5855, 2023.
- [35] Rico Sennrich, Barry Haddow, and Alexandra Birch. Neural machine translation of rare words with subword units. *arXiv preprint arXiv:1508.07909*, 2015.
- [36] Hamid R Sheikh, Muhammad F Sabir, and Alan C Bovik. A statistical evaluation of recent full reference image quality assessment algorithms. *IEEE Transactions on Image Processing*, 15(11):3440–3451, 2006.
- [37] Hengcan Shi, Munawar Hayat, Yicheng Wu, and Jianfei Cai. Proposalclip: Unsupervised open-category object proposal generation via exploiting clip cues. In *Proceedings of the IEEE/CVF Conference on Computer Vision and Pattern Recognition*, pages 9611–9620, 2022.
- [38] Suhas Srinath, Shankhanil Mitra, Shika Rao, and Rajiv Soundararajan. Learning generalizable perceptual representations for data-efficient no-reference image quality assessment. In *Proceedings of the IEEE/CVF Winter Conference on Applications of Computer Vision*, pages 22–31, 2024.
- [39] Shaolin Su, Qingsen Yan, Yu Zhu, Cheng Zhang, Xin Ge, Jinqiu Sun, and Yanning Zhang. Blindly assess image quality in the wild guided by a self-adaptive hyper network. In *Proceedings of the IEEE/CVF Conference on Computer Vision and Pattern Recognition*, pages 3667–3676, 2020.
- [40] Wei Sun, Xiongkuo Min, Danyang Tu, Siwei Ma, and Guangtao Zhai. Blind quality assessment for in-the-wild images via hierarchical feature fusion and iterative mixed database training. *IEEE Journal of Selected Topics in Signal Processing*, 2023.
- [41] Bart Thomee, David A Shamma, Gerald Friedland, Benjamin Elizalde, Karl Ni, Douglas Poland, Damian Borth, and Li-Jia Li. Yfcc100m: The new data in multimedia research. *Communications of the ACM*, 59(2):64–73, 2016.
- [42] Phong V. Vu and Damon M. Chandler. A fast wavelet-based algorithm for global and local image sharpness estimation. *IEEE Signal Processing Letters*, 19(7):423–426, 2012.
- [43] Hui Wang, Guangcheng Wang, Wenjun Xia, Ziyuan Yang, Hui Yu, Leyuan Fang, and Yi Zhang. Blind image quality assessment via deep response feature decomposition and aggregation. *IEEE Journal of Selected Topics in Signal Processing*, 2023.
- [44] Jianyi Wang, Kelvin CK Chan, and Chen Change Loy. Exploring clip for assessing the look and feel of images. In *Proceedings of the AAAI Conference on Artificial Intelligence*, volume 37, pages 2555–2563, 2023.
- [45] Zhenda Xie, Zheng Zhang, Yue Cao, Yutong Lin, Jianmin Bao, Zhuliang Yao, Qi Dai, and Han Hu. Simsim: a simple framework for masked image modeling. In *2022 IEEE/CVF Conference on Computer Vision and Pattern Recognition*, pages 9643–9653, 2022.
- [46] Jingtao Xu, Peng Ye, Qiaohong Li, Haiqing Du, Yong Liu, and David Doermann. Blind image quality assessment based on high order statistics aggregation. *IEEE Transactions on Image Processing*, 25(9):4444–4457, 2016.
- [47] Zipeng Xu, Tianwei Lin, Hao Tang, Fu Li, Dongliang He, Nicu Sebe, Radu Timofte, Luc Van Gool, and Errui Ding. Predict, prevent, and evaluate: Disentangled text-driven image manipulation empowered by pre-trained vision-language model. In *Proceedings of the IEEE/CVF Conference on Computer Vision and Pattern Recognition*, pages 18229–18238, 2022.
- [48] Peng Ye, Jayant Kumar, Le Kang, and David Doermann. Unsupervised feature learning framework for no-reference image quality assessment. In *Proceedings of the IEEE/CVF Conference on Computer Vision and Pattern Recognition*, pages 1098–1105. IEEE, 2012.
- [49] Zhenqiang Ying, Haoran Niu, Praful Gupta, Dhruv Mahajan, Deepti Ghadiyaram, and Alan Bovik. From patches to pictures (paq-2-piq): Mapping the perceptual space of picture quality. In *Proceedings of the IEEE/CVF Conference on Computer Vision and Pattern Recognition*, pages 3575–3585, 2020.
- [50] Yike Yuan, Xinghe Fu, Yunlong Yu, and Xi Li. Densdino: Boosting dense self-supervised learning with token-based point-level consistency. In *Proceedings of the Thirty-Second International Joint Conference on Artificial Intelligence, IJCAI-23*, pages 1695–1703, 2023.
- [51] Hui Zeng, Lei Zhang, and Alan C Bovik. A probabilistic quality representation approach to deep blind image quality prediction. *arXiv preprint arXiv:1708.08190*, 2017.
- [52] Weixia Zhang, Kede Ma, Jia Yan, Dexiang Deng, and Zhou Wang. Blind image quality assessment using a deep bilinear convolutional neural network. *IEEE Transactions on Circuits and Systems for Video Technology*, 30(1):36–47, 2018.
- [53] Weixia Zhang, Kede Ma, Guangtao Zhai, and Xiaokang Yang. Uncertainty-aware blind image quality assessment in the laboratory and wild. *IEEE Transactions on Image Processing*, 30:3474–3486, 2021.
- [54] Weixia Zhang, Guangtao Zhai, Ying Wei, Xiaokang Yang, and Kede Ma. Blind image quality assessment via vision-language correspondence: A multitask learning perspective. In *Proceedings of the IEEE/CVF Conference on Computer Vision and Pattern Recognition*, pages 14071–14081, 2023.
- [55] Kai Zhao, Kun Yuan, Ming Sun, Mading Li, and Xing Wen. Quality-aware pre-trained models for blind image quality assessment. In *Proceedings of the IEEE/CVF Conference on Computer Vision and Pattern Recognition*, pages 22302–22313, June 2023.
- [56] Yiwu Zhong, Jianwei Yang, Pengchuan Zhang, Chunyu Li, Noel Codella, Liunian Harold Li, Luowei Zhou, Xiyang Dai, Lu Yuan, Yin Li, et al. Regionclip: Region-based language-image pretraining. In *Proceedings of the IEEE/CVF Conference on Computer Vision and Pattern Recognition*, pages 16793–16803, 2022.
- [57] Bolei Zhou, Agata Lapedriza, Aditya Khosla, Aude Oliva, and Antonio Torralba. Places: A 10 million image database for scene recognition. *IEEE Transactions on Pattern Analysis and Machine Intelligence*, 40(6):1452–1464, 2017.
- [58] Chong Zhou, Chen Change Loy, and Bo Dai. Extract free dense labels from clip. In *European Conference on Computer Vision*, pages 696–712. Springer, 2022.
- [59] Fei Zhou, Rongguo Yao, Guangsen Liao, Bozhi Liu, and Guoping Qiu. Visual saliency via embedding hierarchical knowledge in a deep neural network. *IEEE Transactions on Image Processing*, 29:8490–8505, 2020.
- [60] Zehong Zhou, Fei Zhou, and Guoping Qiu. Blind image quality assessment based on separate representations and adaptive interaction of content and distortion. *IEEE Transactions on Circuits and Systems for Video Technology*, Early Access:1–14, 2023.
- [61] Zehong Zhou, Fei Zhou, and Guoping Qiu. Collaborative auto-encoding for blind image quality assessment. *arXiv preprint arXiv:2305.14684*, 2023.
- [62] Hancheng Zhu, Leida Li, Jinjian Wu, Weisheng Dong, and Guangming Shi. Metaiqa: Deep meta-learning for no-reference image quality assessment. In *Proceedings of the IEEE/CVF Conference on Computer Vision and Pattern Recognition*, pages 14143–14152, 2020.